

X-Ray Photoelectron, Infrared, and Raman Spectroscopy Studies of Novel Submicrometric Poly[(methacrylato)aluminum(III)]

Alfredo R. Vilchis-Nestor,¹ Víctor Sánchez-Mendieta,¹ Fernando Ureña-Nuñez,² Rafael López-Castañares,¹ Jorge A. Ascencio^{1,3}

¹Facultad de Química, Universidad Autónoma del Estado de México. Paseo Colón y Paseo Tollocan. Apartado Postal A-20, C.P. 50120, Toluca, México

²Gerencia de Ciencia Básicas, Instituto Nacional de Investigaciones Nucleares, Km 36.5, carretera México-Toluca, Ocoyoacac, Estado de México 52045, México

³Instituto Mexicano del Petróleo, Eje Central Lázaro Cárdenas 152, Col. San Bartolo Atepehuacan, C.P.07730, México DF, México

Received 11 September 2006; accepted 23 April 2006

DOI 10.1002/app.24753

Published online in Wiley InterScience (www.interscience.wiley.com).

ABSTRACT: Poly[(methacrylato)aluminum(III)] was prepared by applying γ -radiation to the corresponding aluminum(III) methacrylate monomer. Scanning electron microscopy images show pellets of ~ 500 nm for the aluminum(III) methacrylate monomer, and submicrometric fibers-made granules for the aluminum-containing polymers. X-ray photoelectron spectroscopy measurements reveal two peaks in the Al 2p core-level spectra of the monomer and of the poly[(methacrylato)aluminum(III)], which means that two different coordination modes for the Al(III) ions might be present in these compounds. Infrared and Raman spectroscopy studies confirmed that the structure for this novel co-

ordination polymer consists of hexa-coordinated Al(III) ions linked by the carboxylate groups of methacrylate ligands, along with hydroxyl groups and coordinated water, in a combination of monodentate and bridging bidentate coordination modes. Hence, combination of spectroscopic methods is a helpful tool to get valuable information on the structure of nonmacrocrystalline coordination polymers. © 2006 Wiley Periodicals, Inc. *J Appl Polym Sci* 102: 5212–5223, 2006

Key words: metal–polymer complexes; γ -radiation polymerization; X-ray photoelectron spectroscopy; FTIR spectroscopy; Raman spectroscopy

INTRODUCTION

Polymer structures in which a metal ion is included, in compounds known as coordination polymers, show many prominent features, for example, redox properties, magnetism, conductivity, gas adsorption, or anion exchange.^{1–3} Metal-containing polymers acquire specific physical–mechanical features,¹ they turned out to be efficient and selective catalysts for various reactions^{4,5} and they can have biocide activity, among other useful properties.⁶ Two general approaches are the most widely used in the synthesis of coordination polymers.⁷ In one method, metal ions are attached to a readily available polymer by an appropriate reaction. The second technique consists of synthesizing a metal-containing monomer and then polymerizing that monomer. Reports on this subject include the reaction

between metallic salts and poly(acrylic acid) and poly(methacrylic acid) to get a metal-containing monomer as precursor of a coordination polymer.^{8–10} Metal-containing monomers are usually polymerized in solution, with peroxides or azocompounds as catalysts^{11–13}; however, γ -radiation can also be applied over a metal-containing monomer in solid phase to initiate the polymerization reaction. The efficiency of γ -radiation relies on its capability of penetration, control of the polymerization ratio as a function of the applied dose, high conversions in short reaction times, and further purification processes are not required because there is no contamination by a catalyst or subproducts.¹⁴ Research in coordination polymers has focused mainly on properties of bulk solids. Recently, controlling the growth of the coordination polymers under spatial confinement has resulted in production of nanocompounds.^{15,16} It has become more important to investigate the unexpected chemical and physical properties of nanometric or submicrometric coordination polymers, since their possible interesting size- and shape-dependent properties are still unexplored. Nevertheless, reports about preparing coordination polymers on a nanometer or submicrometric scale have been few to date.^{17,18} A general problem in the characterization

Correspondence to: V. Sánchez-Mendieta (vsm@uaemex.mx).

Contract grant sponsor: Universidad Autónoma del Estado de México (project 1950/2004-2), Instituto Nacional de Investigaciones Nucleares (ININ), and Instituto Mexicano del Petróleo.

of coordination polymers arises because of the extreme intractability of many of these materials, and the consequent lack of available structural information. In addition, owing to the difficulty of obtaining single crystals, relatively few structure determinations have been carried out on coordination polymers, necessitating the use of indirect methods of structural characterization.¹⁹ Although poly(methacrylic acid) has been known for many years,²⁰ to date, few metal–poly(methacrylate) coordination polymers have been synthesized,^{9,10} none of them can be obtained as a single crystal compound; consequently, still very little is known about the structure of these materials; moreover, there are relatively few recent studies based on infrared spectroscopy, reporting on the coordination geometries in polycarboxylate–metal ion complexes.^{10,21} Therefore, it is essential to explore the application of experimental methods to study the structural characteristics of these potential functional materials.

In this article, we report an easy synthesis of the microcrystalline and submicrometric novel poly[(methacrylate)aluminum(III)] (PMAAI), and its structural characterization employing X-ray photoelectronic, IR, and Raman spectroscopic methods, and scanning electron microscopy, as well as electron paramagnetic resonance (EPR) and thermogravimetric analysis.

EXPERIMENTAL PROCEDURE

Synthesis of aluminum(III) methacrylate

Methacrylic acid (MAc) (Sigma-Aldrich, Mexico), NaHCO₃ (Sigma-Aldrich, Mexico), and AlCl₃ · 6H₂O (J. T. Baker, Mexico), all of them of reagent grade, were employed without any further purification. De-ionized water was used to prepare all the solutions in this work. Briefly, NaHCO₃ (aq) (9.91 g, 117.9 mmol) was added to an equivalent amount of MAc (10.15 g, 117.9 mmol), and the solution was stirred for 30 min at room temperature. Then, AlCl₃ · 6H₂O (9.49 g, 39.3 mmol) was

poured, while stirring, to the freshly prepared sodium methacrylate (MANa) solution. This mixture was stirred for 1 h at 60°C. MAAI precipitated as a white powder, which was isolated by filtration, washed thoroughly with de-ionized water, and vacuum-dried.

Polymerization of MAAI

About 1 g of monomer was placed in a glass tube, which was evacuated and then vacuum-sealed. Irradiation of MAAI was carried out at room temperature in a Gammacell-220 (AECL), having a ⁶⁰Co γ-ray source with a dose rate of 0.25 kGy/h. Doses of 10, 20, 30, 40, and 50 kGy were applied to the monomer. PMAAI showed insolubility to most common solvents.

Characterization methods

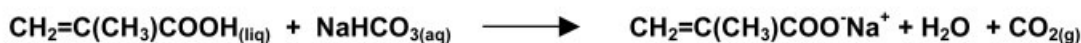
A Perkin–Elmer 2380 atomic absorption spectrophotometer was used to calculate the monomer yield with a standard curve of sodium from 5 to 25 ppm, in de-ionized water.

Monomer and polymer morphologies were analyzed and imaged with a PHILIPS XL-30 scanning electron microscope (SEM) at 25 kV equipped with a detector for energy dispersive X-ray analysis (EDAX). Samples were fixed on a support with a copper film and sputter-coated with gold to a thickness of ~ 200 Å.

EPR analyses were carried out at room temperature using a Varian E-15 electron paramagnetic spectrometer operating at a frequency of 9.5 GHz. The instrument settings were as follows: a magnetic field of 330 mT; a scan range of 40 mT; a scan time of 8 min; a magnetic field modulation amplitude of 0.1 mT; a modulation frequency of 100 kHz; and a microwave power of 5 mW.

FTIR spectra were obtained with a Nicolet-FTIR 550 spectrophotometer using KBr pellets. Raman measurements were made with a Jobin Yvon Raman microscope Olympus BX41 in a frequency range of 4000–400 cm⁻¹.

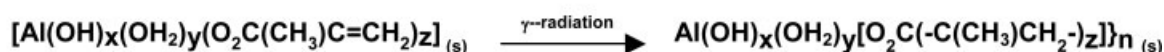
Reaction 1



Reaction 2



Reaction 3



Scheme 1 Schematic representation of the reactions involved in PMAAI synthesis.

The excitation source was a He-Ne ion laser, and the spectra were collected using the 632.8 nm radiation.

Thermal degradation of monomer and polymer samples were performed using a TA Instruments TGA-51 apparatus, calibrated with a standard of calcium oxide. Experiments were conducted from 20 to 800°C, with a heating rate of 10°C/min, under nitrogen atmosphere; sample weight was around 10 mg.

X-ray photoelectron spectroscopy (XPS) experimental set up was done with a VG Microtech MultiLab ESCA 2000. The UHV system with a CLAM4 MCD electron analyzer and Mg K α ($h\nu = 1253.6$ eV) X-ray source was operated at 15 kV and 20 mA. The incidence angle was 55° with respect to the surface; survey and high-resolution narrow scan were done to constant pass energy of 50 and 20 eV, respectively. The SDPv 4.1 software was used to analyze the experimental results. The surface chemical composition was determined from the corresponding peak area by using the correc-

tion of the relative sensitivity factor (RSF) reported by Scofield.²² Corrections of charging of the scanned elements for all samples were carried out taking the position of sapphire (Al₂O₃) and poly(methacrylic acid) as reference.²³ The vacuum level during measurements was less than 1×10^{-8} mb. The peak positions were referenced to the background of Ag 3d^{5/2} photopeak at 367.8 eV. The full width at half-maximum (FWHM) was maintained at 1.0 eV using Ag 3d^{5/2}.

RESULTS AND DISCUSSION

Synthesis

Aluminum(III) methacrylate (MAAI) was synthesized following the method reported by Galvan et al.,²⁴ where iron(III) methacrylate was obtained, and then polymerized with γ -radiation, having high yields of this monomer in a two-step reaction (see Scheme 1,

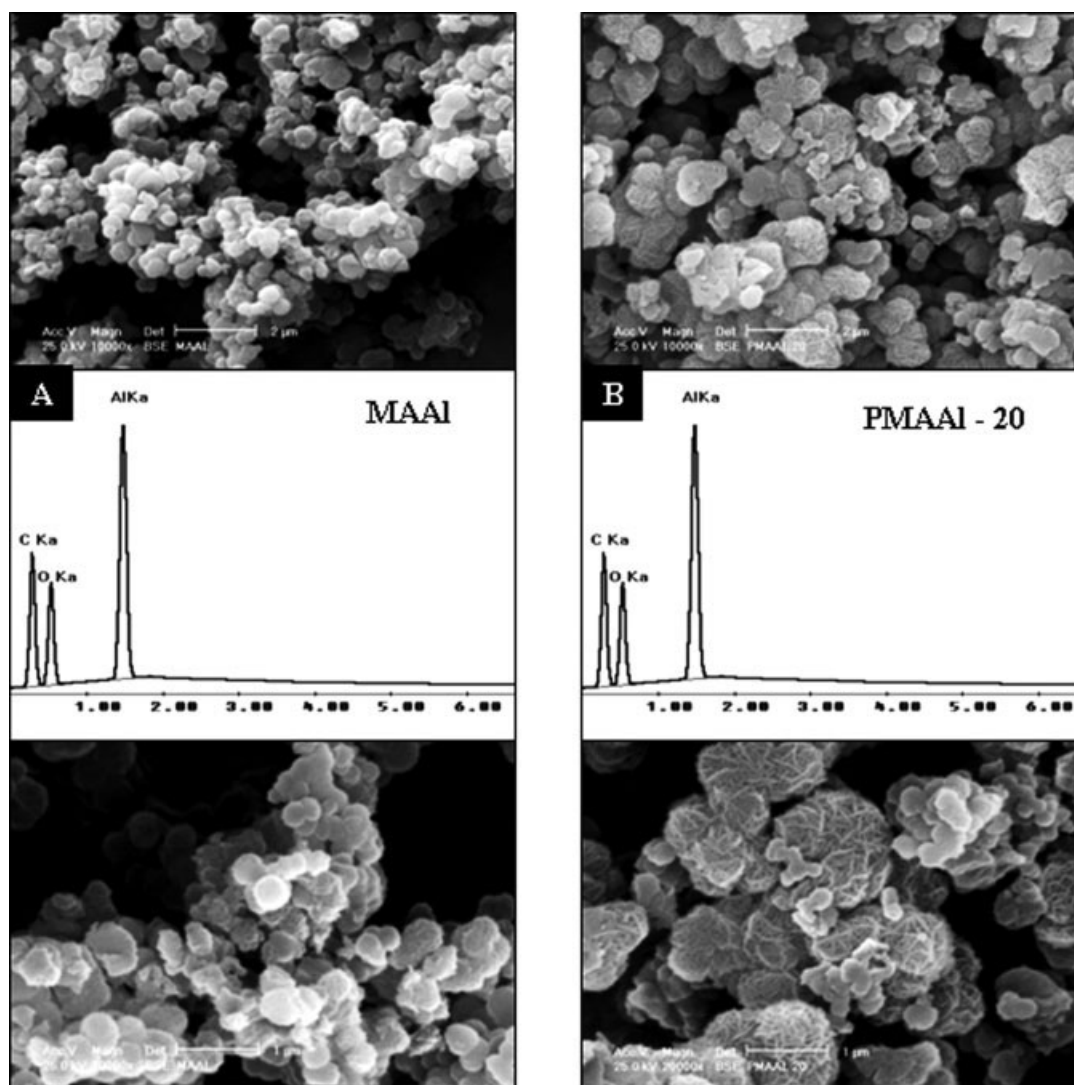


Figure 1 EDAX spectra and SEM images showing the chemical composition and the morphologies of (A) MAAI and (B) PMAAI-20 kGy.

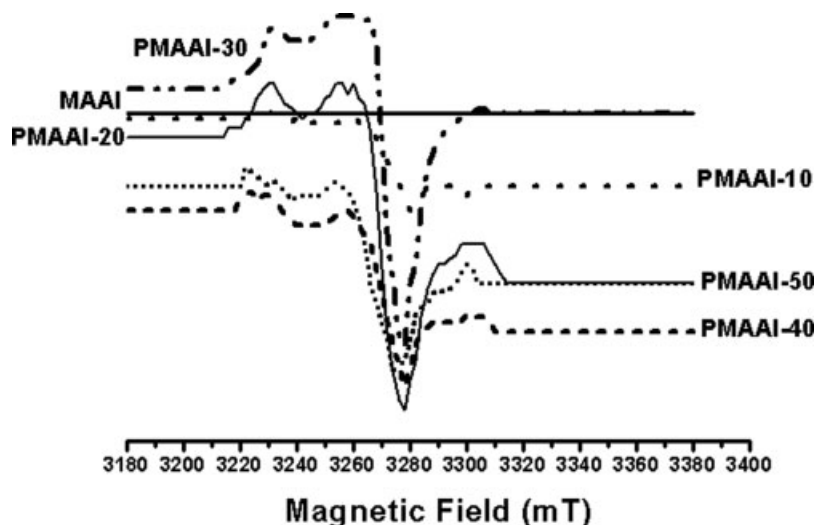


Figure 2 EPR spectra of MAAI and PMAAI obtained at 10, 20, 30, 40, and 50 kGy of γ -radiation doses.

below). A yield of 89.1% was obtained in MAAI synthesis, as determined by AA spectrophotometry. Doses of 10, 20, 30, 40, and 50 kGy of γ -ray radiation were applied to the monomer, with a dose rate of 0.25 kGy/h.

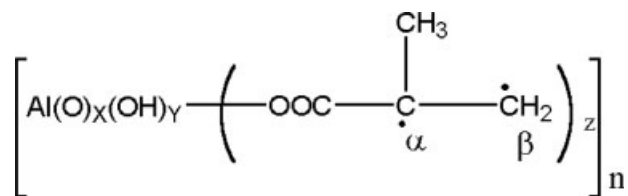
Scanning electron microscopy

EDAX studies showed that only carbon ($\sim 67\%$), oxygen ($\sim 26\%$), and aluminum ($\sim 7\%$), were found on MAAI and all PMAAI samples (Fig. 1). Scanning electron microscopy images in Figure 1 show the morphological differences between MAAI and PMAAI, irradiated at 20 kGy (PMAAI-20). It can be observed that the pellets of the MAAI [Fig. 1(A)] are closer to a spherical shape than those of PMAAI-20 [Fig. 1(B)], and with diameters of ~ 500 nm. Unlike the monomer, the morphology of PMAAI-20 resembles fibers hank [Fig. 1(B)], confirming, in such a way, that polymer formation has occurred. Similar fiber-type morphology has been obtained in scanning electron microscopy studies of poly[(methacrylate)zinc(II)].²⁵ Moreover, PMAAI-20 granules have sizes that range from 300 nm to a bit more than 1 μm , approximately. Small pellets observed in Figure 1(B) are believed to have come from the degradation of the polymer, and consequent oligomer formation, due to the action of γ -ray radiation, which is a common event when this type of radiation is employed to polymerize.²⁶

Electron paramagnetic resonance

Figure 2 shows the electron paramagnetic resonance (EPR) spectra of MAAI and PMAAI samples. As can be observed, there is no signal for MAAI; however, a well-defined signal centered at around 330 mT can

be observed for PMAAI samples, which can be associated to the propagative radical shown below:



This radical has been studied previously by Sakai.²⁷ Furthermore, Ichikawa²⁸ found that the absorption of radiation energy by methacrylate polymers always involves the formation of this tertiary radical. The different EPR signal intensities of the spectra in Figure 2 are associated to the amount of radicals produced for each applied dose. Figure 2 shows how the EPR signal intensity increases as a function of the applied dose. It must be pointed out that EPR measurements were carried out immediately after irradiations and, that no EPR signal was found after ~ 40 h of irradiation, as can be observed in Figure 3 for PMAAI-20.

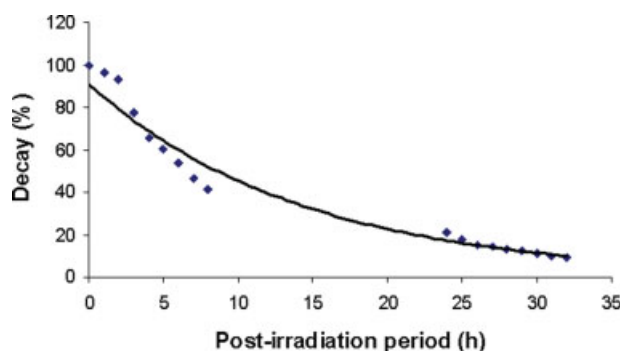


Figure 3 Decay of the EPR signal of PMAAI-20. [Color figure can be viewed in the online issue, which is available at www.interscience.wiley.com.]

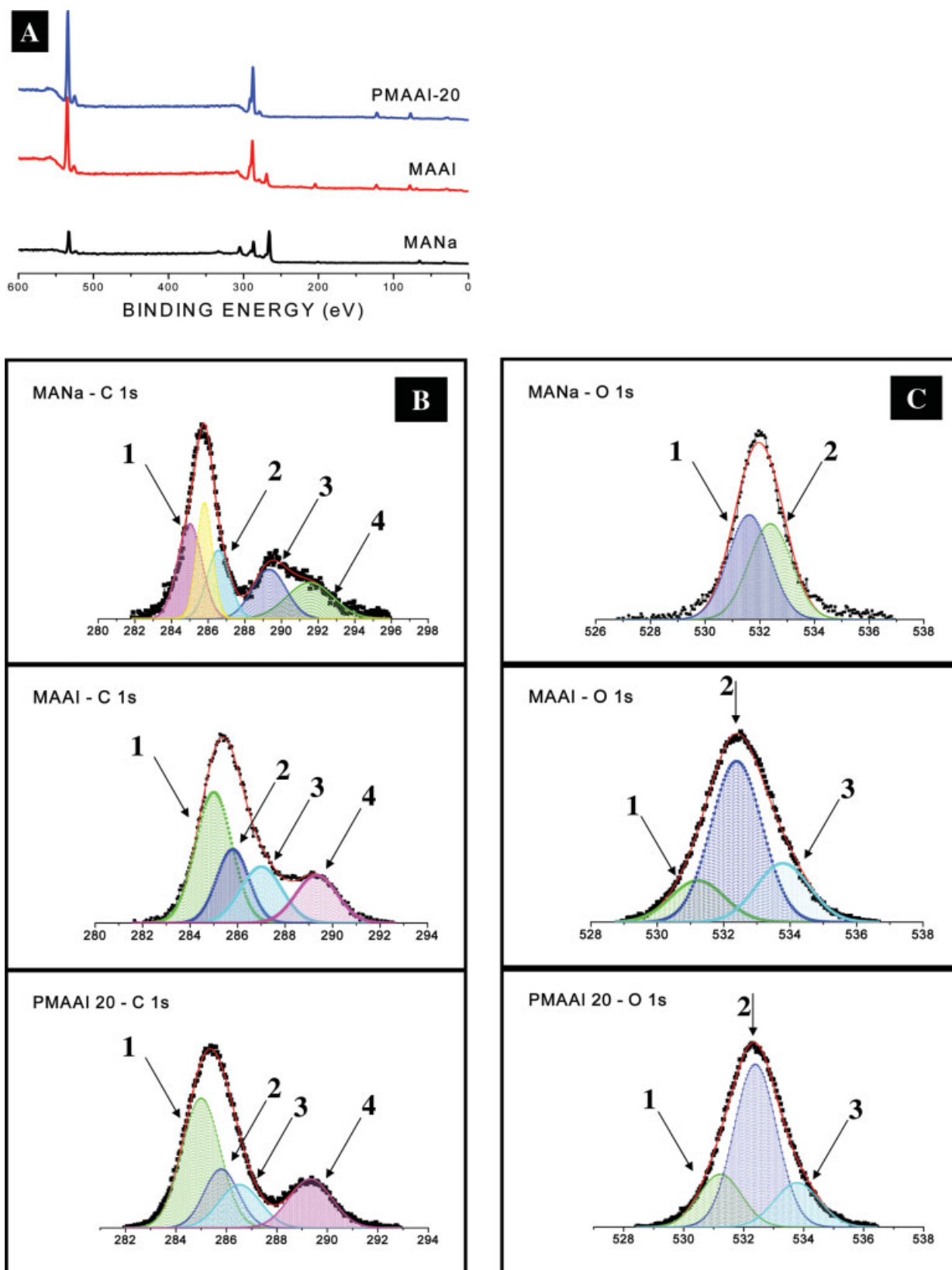


Figure 4 XPS spectra of MANa, MAAI, and PMAAI 20 kGy; (A) survey spectra; (B) C 1s spectra; (C) O 1s spectra. (1B) 285 eV corresponds to CH_2 and CH_3 ; (2B) 285.8 eV corresponds to $-(\text{CH}_3)\text{C}=\text{}$; (3B) 287 eV corresponds to $\text{C}-\text{O}$ in a bridging complex; (4B) 289.3 eV corresponds to COO^- in monodentate complex for MAAI and PMAAI. (1C) 531.6 eV and (3C) 533.8 eV correspond to $\text{C}=\text{O}$ and $\text{C}-\text{O}$ in monodentate complex, respectively; (2C) 532.3 eV corresponds to $\text{C}-\text{O}$ in bridging complex. [Color figure can be viewed in the online issue, which is available at www.interscience.wiley.com.]

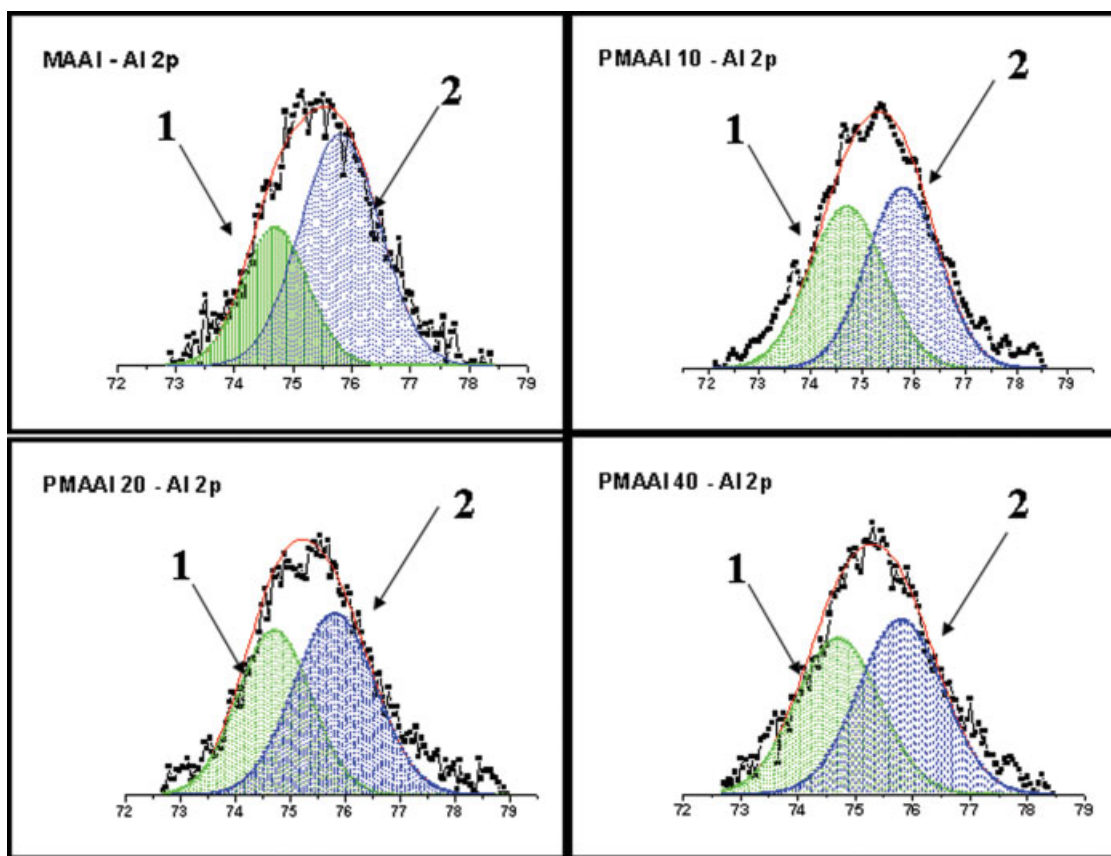


Figure 5 XPS Al 2p spectra of MAAI, PMAAI-10, PMAAI-20, and PMAAI-40. [Color figure can be viewed in the online issue, which is available at www.interscience.wiley.com.]

X-ray photoelectron spectroscopy measurements

Figure 4(A) shows the X-ray photoelectron spectroscopy (XPS) survey of MANa, MAAI, and PMAAI-20. The expected elements C, O, and Al were detected; from this survey spectrum, an Al elemental concentration of $\sim 7.1\%$ was found in all polymers. XPS results for MANa, MAAI, and PMAAI-20 are reported in Figures 4(B) and 4(C). Four peaks can fit the high resolution XPS spectra of C 1s core-level for MANa: 285, 285.8, 287, and 289.3 eV [Fig. 4(B)], which can be assigned to the carbon in the CH_3 or CH_2 , $\text{C}=\text{C}$, $\text{COO}^- \text{Na}^+$, and COOH , respectively.²³ The four peaks are also observed in the MAAI and PMAAI-20 C 1s core-level spectra [Fig. 4(B)]. The O 1s core-level spectra [Fig. 4(C)] change from two-peak fit spectrum for MANa to three-peak fit spectra for MAAI and PMAAI-

20. This change can be attributable to the formation of two different coordination structures between the aluminum ions and carboxylate groups (vide infra). In addition, the peak at 531.4 eV [Fig. 4(C)] suggest the presence of $-\text{OH}$ groups bound to aluminum(III).²⁹ In Figure 5, it is shown that all XPS spectra of Al 2p can be fitted to two peaks³⁰: 74.7 and 75.8 eV, which suggests that after the aluminum(III) complex formation, two coordination environments are involved for the aluminum ions.

IR and Raman spectroscopy

Carboxylate groups can coordinate to a metal ion in three possible ways, which are shown in Figure 6. Structure I corresponds to monodentate complex,

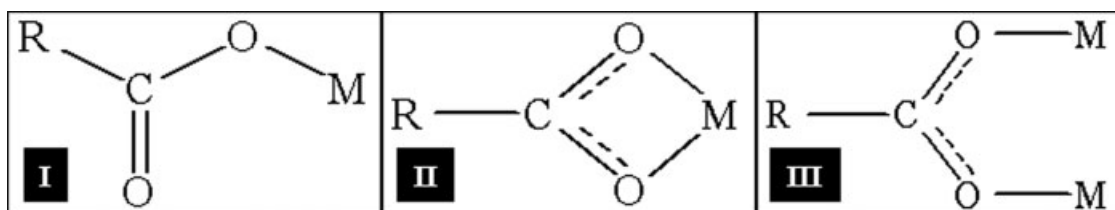


Figure 6 Representations of the coordination modes of carboxylate ligands to metal ion: (I) mono-dentate, (II) chelating bi-dentate, and (III) bridging-bidentate.

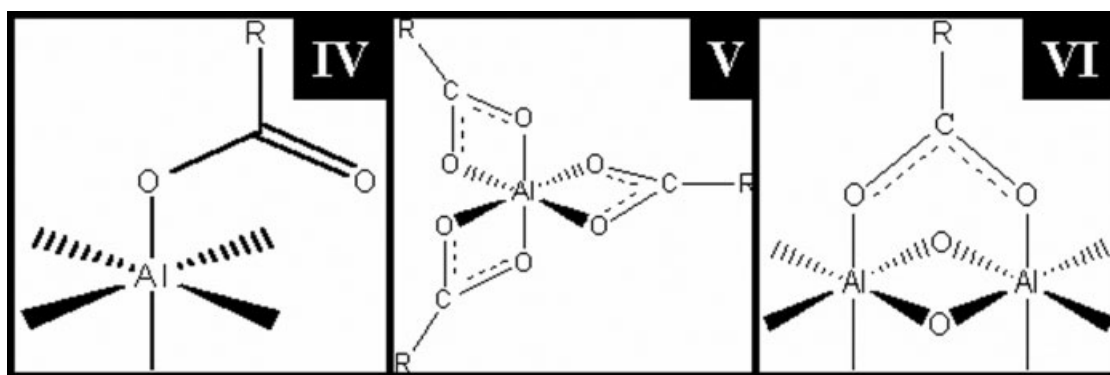


Figure 7 Representations of the coordination modes of carboxylate ligands to aluminum(III) ion: (IV) mono-dentate, (V) chelating bi-dentate, and (VI) bridging-bidentate.

where the oxygen atoms of three carboxylate groups coordinate to a metal ion using single bonds. Structure II shows a chelating symmetrical bi-dentate fashion; while, structure III corresponds to a bridging bidentate complex. These two last coordination modes involve a bi-dentate binding; i.e., both oxygen atoms of a carboxylate group take part in the coordination. In chelating-bidentate coordination, both oxygen atoms are bound to a metal ion, whereas, in the bridging coordination, the two oxygen atoms are bound to two different metal ions.^{31,32} These type of coordination modes for carboxylate-containing ligands have been reported previously.³³ For aluminum(III)-carboxylate compounds, $[\text{Al}(\text{O}_2\text{CR})_3]$, a chelating bi-dentate coordination (Fig. 7, V) has been proposed.^{34,35} Although, there has not been spectroscopic evidence for this mode of coordination to aluminum(III). Most recently, Leman et al.³⁶ demonstrated that in aluminum(III)-carboxylate compounds, using triazene-type ligands, there is no evidence of the chelating bi-dentate fashion in the coordination sphere of Al ions. In addition, Barron et al.^{37,38} in their profound spectroscopic studies about aluminum(III)-carboxylate complexes found only monodentate (Fig. 7, IV) and bridging bidentate (Fig. 7, VI) coordination modes.

FTIR and Raman spectroscopy can differentiate among these different coordination modes, specifically on the carbonyl stretching frequencies.^{10,33} Complete studies of the corresponding absorption bands have been done for acetate complexes of known structure.³⁹ Figure 8 shows the IR absorption spectrum of MAc. Characteristic bands reported for MAc appear in that spectrum.⁴⁰ Bands related to CH_3- (Fig. 8) appear at 2930 cm^{-1} , which results from the C—H stretching in C— CH_3 type compounds. The bands in the bending region at 947 and 810 cm^{-1} , associated to the vinylidene group $\text{C}=\text{CH}_2$, correspond to the CH_2 out-of-plane wagging. Bands due to $-\text{COOH}$ (Fig. 8) can be assigned as follows: a broad band between 3300 and 2400 cm^{-1} (O—H stretching vibration), a strong band at 1698 cm^{-1} (C=O stretch in carboxylic

acid), and also strong bands at 1299 and 1204 cm^{-1} (C—O stretching). Usually, two bands, arising from C—O stretching and O—H bending, appear in the spectra of carboxylic acids near 1320 – 1210 cm^{-1} and 1440 – 1395 cm^{-1} , respectively.⁴¹ These bands involve some interaction between C—O stretching and in-plane C—O—H bending. The more intense band, near 1315 – 1280 cm^{-1} , is normally referred to as the C—O stretching band and usually appears as a doublet in the spectra as can be seen in Figure 8. This has been found particularly for dimer compounds.⁴²

Figure 9 shows the FTIR and Raman spectra for MAAI. In the IR spectrum a weak broad band from 3600 to 3100 cm^{-1} can be observed, which replaces the strong-broad band from 3300 to 2400 cm^{-1} in MAc spectrum (Fig. 8). The band for $-\text{COOH}$ stretching vibration at 1697 cm^{-1} found in the MAc spectrum, disappeared because of carboxylate ion formation, and two new bands emerge. This behavior is typically observed when the carboxylate anion is coordinated

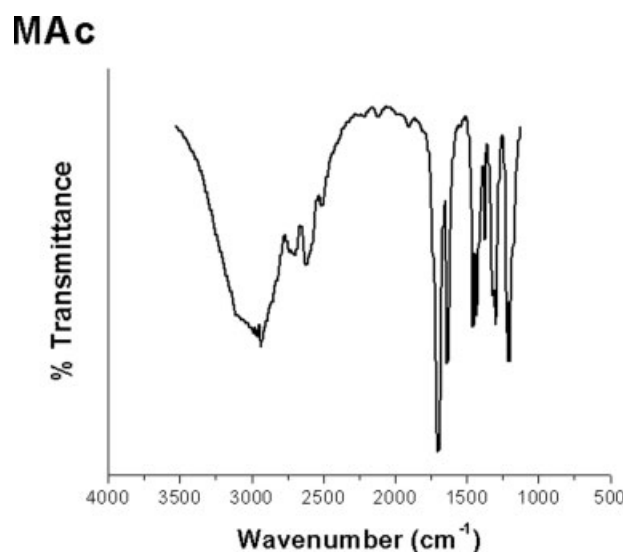


Figure 8 IR spectrum for methacrylic acid.

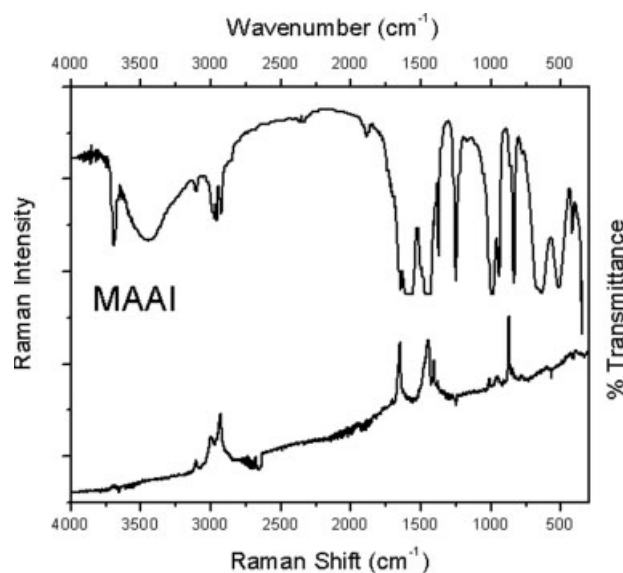


Figure 9 IR and Raman spectra for MAAI.

to a metal.⁴³ Bands at 1590 and 1455 cm^{-1} can be associated to the asymmetric and symmetric stretching vibration of the COO^- , respectively. Following the Deacon and Philips procedure³⁹ to study carboxylate complexes by IR, the MAAI exhibits a Δ value [$V_{\text{asymmetric}}(\text{COO}^-) - V_{\text{symmetric}}(\text{COO}^-)$] of 135, which corresponds to the bridging bi-dentate complexes (Fig. 7, VI). A detailed summary of the main infrared and Raman bands for MAAI and PMAAI-20 are shown in Table I.

The FTIR and Raman spectra of PMAAI obtained with 20 kGy (PMAAI-20) are shown in Figure 10. Both spectra reveal some common features: (a) the symmetric stretching modes of $-\text{CH}_3$ and CH_2 (either on $=\text{CH}_2$ or $-\text{CH}_2-$) moieties are in the 2850–3050 cm^{-1} frequency region; (b) the $\text{C}=\text{O}$ stretching vibration appears in the 1645–1655 cm^{-1} frequency region; (c) the symmetric CO_2^- stretching vibration is at

1445–1455 cm^{-1} , and (d) a strong band at 940–950 cm^{-1} , which can be attributed to the vibration of an $\text{Al}-\text{O}$ bond. However, Raman spectra do not exhibit a band at 3692 cm^{-1} , which corresponds to the stretching modes of a hydroxyl bound to an aluminum(III) ion, and a weak broad band at 3600–3100 cm^{-1} region coming from $-\text{OH}$ stretching modes. According to Srinivasan et al.,⁴⁴ when hydroxyl groups bound to three octahedrally coordinated aluminum(III) ions, an IR absorption frequency around 3690 cm^{-1} occurs, and this can be assigned to the most acidic hydroxyl on alumina surfaces. In addition, all the IR spectra of the alumoxanes reported by Landry et al.⁴⁵ show an absorption band between 3700 and 3400 cm^{-1} , which is consistent with our results. Furthermore, in the IR spectra there is a band around 1370 cm^{-1} , which can be assigned to either, $-\text{CH}_3$ symmetric deformation or the $\text{C}-\text{O}$ bond vibration for metal-carboxylic complexes that possess a monodentate coordination mode. Nevertheless, the Raman spectra do not have such a band, even though in that region usually the $-\text{CH}_3$ symmetric deformation should appear. Therefore, this confirms that the IR band at 1370 cm^{-1} can be assigned to a $\text{C}-\text{O}$ bond vibration and that PMAAI compounds contain also a monodentate coordination mode.

Hence, the IR spectra of all PMAAI have bands at 1596–1590 cm^{-1} and 1459 cm^{-1} , which is consistent with a bridging bidentate mode of coordination. In addition, IR and Raman spectra of the samples show a band approximately at 1650 cm^{-1} and IR spectra contain one additional band at 1370 cm^{-1} , indicative of monodentate coordination in aluminum-carboxylate complexes.⁴⁵ Similar results were found for $[\text{Me}_2\text{Al}(\mu\text{-O}_2\text{CR})_2]$ and $\text{Al}(\text{O}_2\text{CR})(\text{salen})$ [$\text{R}=\text{CH}_3$, C_5H_{11} , H_2 ($\text{salen}) = \text{N,N}'\text{-ethylenebis}(\text{salicylideneamine})$],⁴⁶ where IR bands, providing evidence of the presence of monodentate and bridging bidentate aluminum(III)-carboxylate compounds, were obtained.

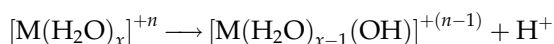
TABLE I
Summary of the Infrared and Raman Bands for Mac, MAAI, and PMAAI-20

Peak assignment	Mac	MAAI		PMAAI-20	
	IR (cm^{-1})	IR (cm^{-1})	Raman (cm^{-1})	IR (cm^{-1})	Raman (cm^{-1})
OH in COOH	3600–3100	N/P ^a	N/P	N/P	N/P
Al–OH stretching	N/P	3692	N/P	3694	N/P
C–H in C– CH_3	2938	2972	2984	2973	2983
C–H in C– CH_2 –C	N/P	N/P	N/P	2927	2929
C=O in COOH	1698	N/P	N/P	N/P	N/P
C=O in COO^- monodentate	N/P	1650	1653	1648	1654
C–O in COO^- monodentate	1375	1374	N/P	1373	N/P
COO^- asymmetric in bridging	N/P	1588	N/P	1587	N/P
COO^- symmetric in bridging	1455 ^b	1449	1453	1443	1454
Al–O bond	N/P	944	952	943	953

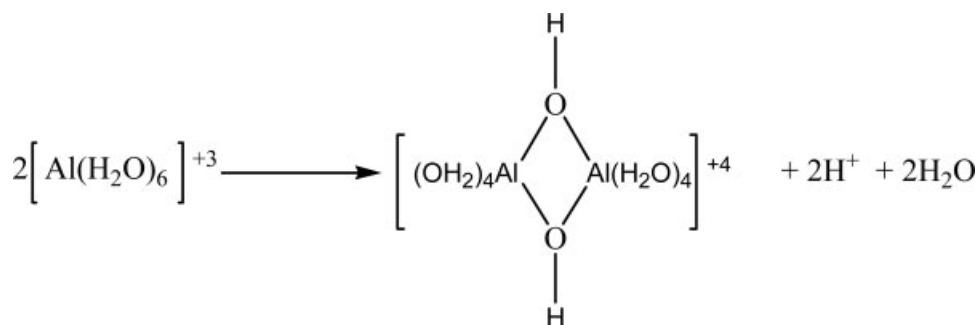
^a N/P, not present.

^b COO^- in COOH.

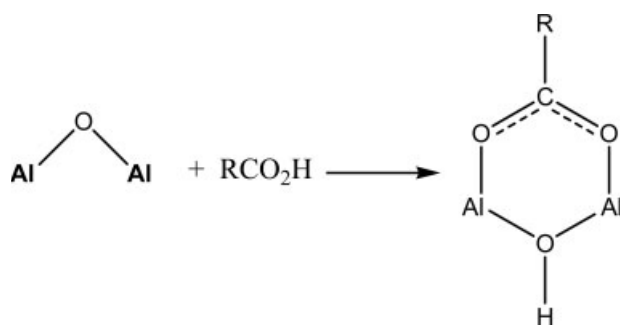
It is well known that water molecules attached to metal ions can have certain acidity, which can give origin to hydroxyl species,



Acidity of aqua ions can vary in concordance to the metal ion to which they are attached, in case of Al ions, $K_a(Al^{3+}) = 1.12 \times 10^{-5}$; hence, solutions of Al(III) ions will usually exhibit an intensive hydrolysis.⁴⁷ The above hydrolysis reaction is the simplest one; however, hydroxyl species can give rise to a dimer at a pH of ~ 5 .

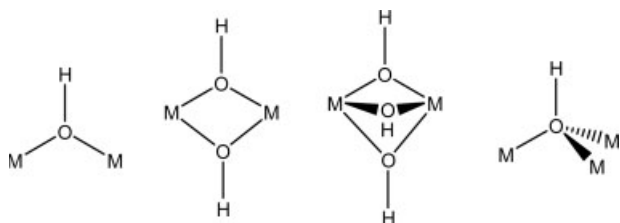


At higher pH values (7–12), polymeric species can be formed, which includes octahedral bridges of Al ions and OH moieties.⁴⁷ Also, protonation of an oxo ligand has been proposed by Barron and coworkers.^{38,45} They found, in their study about the reaction of bohemite with several carboxylic acids, an increase in the number of hydroxyl groups throughout the protonation of oxo ligands as shown in the following reaction,

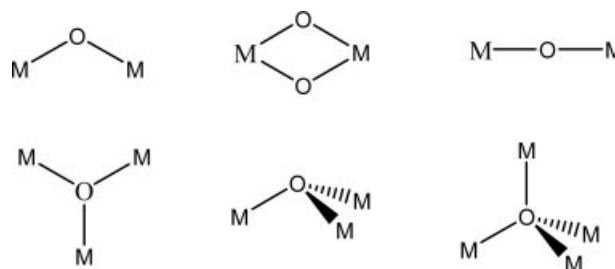


Therefore, presence of water and hydroxyl ligands in PMAAl as a part of the coordination sphere of the Al ions, and accordingly to the method of synthesis employed, was expected.

A common feature of hydroxo complexes is the formation of hydroxo bridges of the following types:



The loss of a second proton from the coordinated water can lead the formation of oxo compounds, which can be of several types:⁴⁷



Exchange of bridge and terminal oxo groups is known to occur in solution. Furthermore, this kind of oxo bonding is not new, oxygen centered triangles are units found widely in so-called "basic" carboxylates and some other bridging anions of many metals. When the metal ion has an oxidation state of +3, as in MAAl and PMAAl, they have the general for-

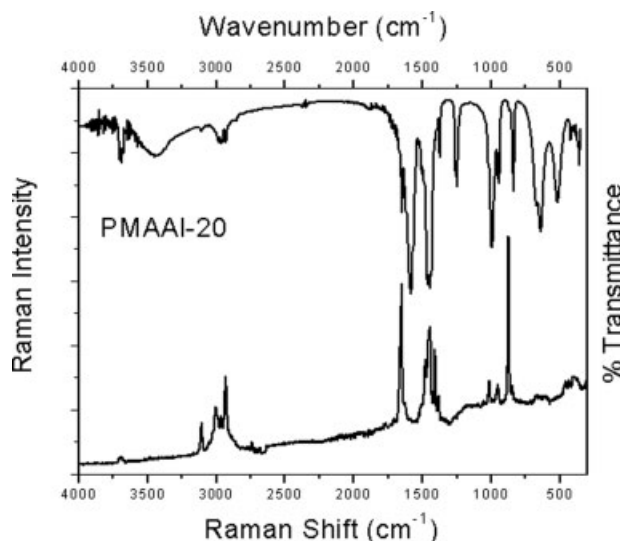


Figure 10 IR and Raman spectra for PMAAl-20.

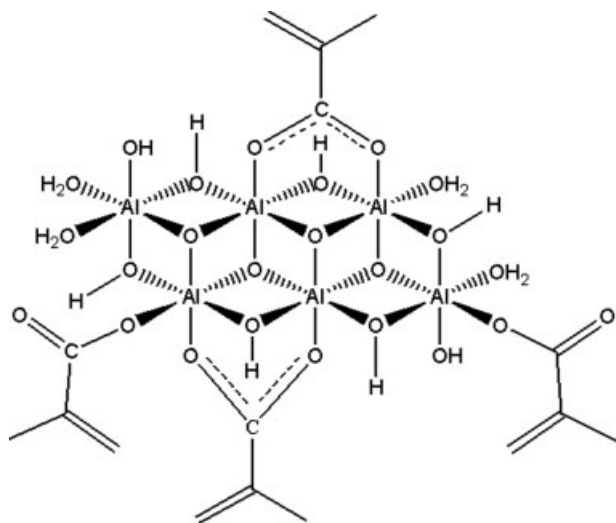
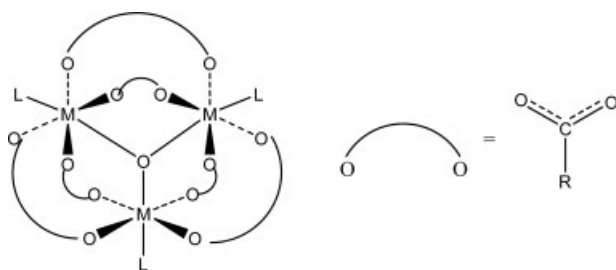


Figure 11 Schematic representation of the possible structure of MAAI.

mula $[M_3O(O_2CR)_6L_3]$, where L is usually a ligand such as H_2O .⁴⁷



According to the previous explanation, and the spectroscopy results obtained, which indicate that the carboxylate of the methacrylate ligands can bind the Al ions in a bridging bidentate mode, and also in a monodentate fashion, a possible representation of a part of MAAI structure is shown in Figure 11. The presence of bridging bidentate carboxylate groups, where a carboxylate links two adjacent aluminum ions is unambiguous, as proved by IR and Raman spectroscopy studies. However, the formation of the carboxylate-aluminum(III) monodentate complex would be rationalized as a part of the MAAI and PMAAI submicrometric particle surface, as it is clear from the XPS analyses, where two different electronic environments for the aluminum(III) ions can be distinguished. A similar aluminum(III)-carboxylate complex structure might be present for the PMAAI obtained at different doses in this study.

Thermogravimetric analysis

TG and DTG curves are shown in Figure 12(a-c) for MAAI, PMAAI-10, and PMAAI-40, respectively. All TGA data are listed in Table II. For all samples,

monomer, and polymers, the first mass loss indicates evaporation of noncoordinated water at around 135°C , which agrees with the results obtained by McNeill and Zulfiqar⁴⁸ and Rufino and Monteiro²¹ for metals salts of poly(methacrylic acid). A further mass loss of 13–18% occurs between 310 and 340°C . Based on results of Landry et al.⁴⁵ and Rufino and Monteiro,²¹ related to thermal studies on bohemita and metallic salts of poly(methacrylic acid), respectively, the second mass loss can be attributed to the dehydration of the aluminum(III) complex. The third

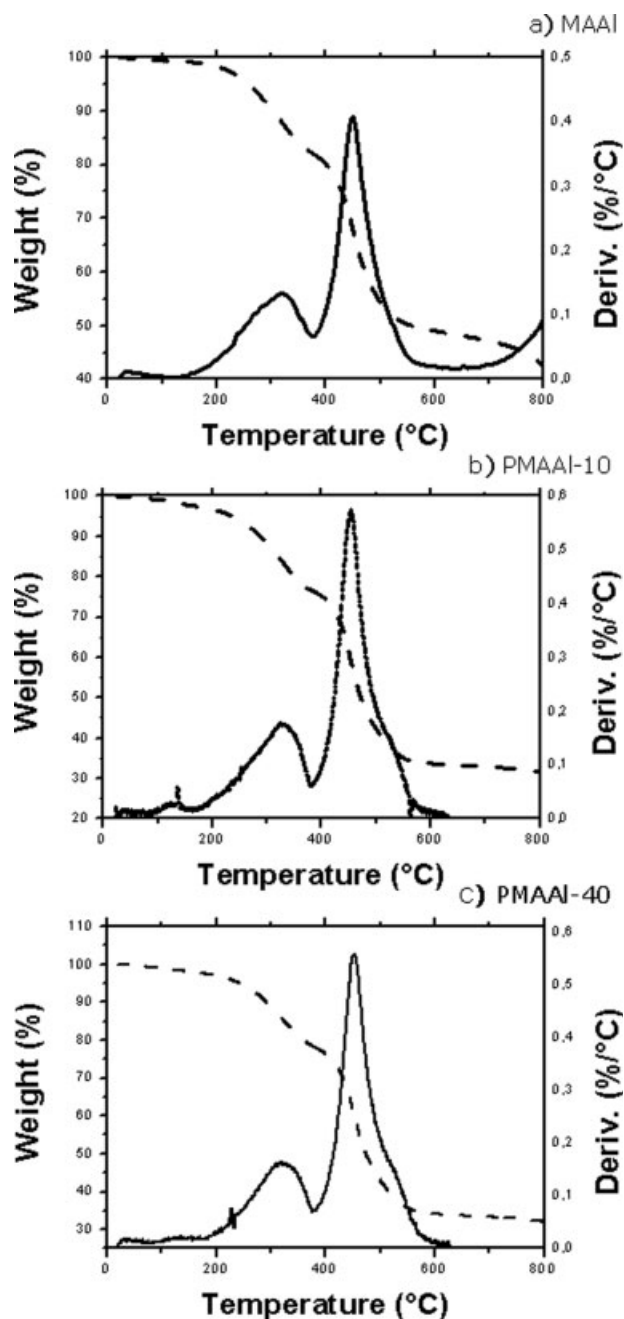


Figure 12 TG and DTG curves of (a) MAAI, (b) PMAAI-10, and (c) PMAAI-40.

TABLE II
Summary of the Temperatures of Mass Loss and Percentage of Residue at 800°C for MAAI and PMAAI's

Sample	Loss temperature (°C)	Weight loss (%)	Residue at 800°C (%)
MAAI	319.2	13.62	42.2
	450.0	40.79	
	136.5	4.28	
PMAAI-10	326.9	17.68	31.5
	453.8	57.10	
	134.6	5.60	
PMAAI-20	334.6	17.57	32.0
	453.8	50.23	
	209.6	6.00	
PMAAI-30	319.2	16.94	31.7
	451.9	57.71	
	226.9	6.28	
PMAAI-40	319.2	16.39	32.0
	453.8	55.56	
	226.9	5.14	
PMAAI-50	319.2	16.74	32.0
	453.8	52.12	

stage occurs above 400°C for all the PMAAI and at 450°C for MAAI. The residual mass, at 800°C, was 42% for MAAI and 32% for PMAAI. The chemical composition of the residue obtained at this last step, and the mechanisms involved in the decomposition process, have been discussed in the literature by McNeill and Zulfiqar⁴⁸ and Zulfiqar and Masud⁴⁹ for transition metal-polymethacrylates complexes.

CONCLUSIONS

Aluminum(III) methacrylate was obtained by an easy synthetic procedure. Polymerization of this monomer was initiated with γ -radiation, producing the novel coordination polymer: poly[(methacrylate)aluminum(III)], PMAAI, which has a submicrometric size. Structural studies by IR and Raman spectroscopy revealed that monodentate and bridging bidentate coordination modes are present in the coordination sphere of the Al ions. Moreover, there are two different coordination spheres for Al ions according to XPS studies. As it is known, many coordination polymers cannot be obtained as single crystals suitable for X-ray diffraction studies; therefore, the use of spectroscopic methods to elucidate the structure of these type of coordination monomer and polymers offers a good alternative to get more insight about these important materials and their potential applications. Therefore, the reported results imply an important perspective for these aluminum(III)-containing polymers to be used as catalysts. Evaluation of PMAAI as catalyst for the dehydration of 2-propanol is currently underway.

The authors want to thank Lazaro Huerta from Instituto de Investigaciones en Materiales, UNAM, and Leticia Carapia from ININ, for their help on XPS and SEM studies, respectively.

References

- Pittman, C.; Carraher, C.; Sheats, J.; Tinken, M.; Zeldin, M. In *Inorganic and Metal-Containing Polymeric Materials*; Sheats, J.; Carraher, C.; Pittman, C.; Zeldin, M.; Currel, B., Eds.; Plenum Press: New York, 1990; Chapter 1.
- Moulton, B.; Zaworotko, M. *Chem Rev* 2001, 101, 1629.
- Patrick, B.; Reiff, W.; Sanchez, V.; Storr, A.; Thompson, R. *Inorg Chem* 2004, 43, 2330.
- Pormogailo, A. D. *Catalysis by Polymer-Immobilized Metal Complexes*; Gordon & Breach: Australia, 1998.
- Guyot, A. *Pure Appl Chem* 1988, 60, 365.
- Zihltsov, S. F.; Nashaeva, V. N. *PhysicoChemical Foundations of Polymer Synthesis and Processing*; Gorkii: Moscow, 1984.
- Odian, G. *Principles of Polymerization*; Wiley: New York, 1991.
- Szalinska, H.; Pietrzak, M.; Janowska, G. *Radiat Phys Chem* 1986, 27, 101.
- Zulfiqar, M.; Hussain, R.; Zulfiqar, S.; Mohammad, D.; McNeill, I. C. *Polym Degrad Stab* 1996, 51, 167.
- Konradi, R.; Rhe, J. *Macromolecules* 2004, 37, 6954.
- Leadbeater, N. E.; Marco, M. *Chem Rev* 2002, 102, 3217.
- Bergbreiter, D. E. *Chem Rev* 2002, 102, 3345.
- Dickerson, T. J.; Reed, N.; Janda, K. *Chem Rev* 2002, 102, 3325.
- Filardo, G.; Caputo, G.; Galia, A.; Calderaro, E.; Spadaro, G. *Macromolecules* 2000, 33, 278.
- Zhon, P.; Xue, D.; Luo, H.; Chen, X. *Nano Lett* 2002, 2, 845.
- Mingotaud, C.; Lafuente, C.; Amiell, J.; Delhaes, P. *Langmuir* 1999, 15, 289.
- Uemura, T.; Kitagawa, S. *J Am Chem Soc* 2003, 125, 7814.
- Yamada, M.; Arai, M.; Kurihara, M.; Sakamoto, M.; Migake, M. *J Am Chem Soc* 2004, 126, 9482.
- Sanchez, V.; Storr, A.; Thompson, R. C. *Can J Chem* 2002, 80, 133.
- Van den Bosch, E.; Keil, Q.; Filipcsei, G.; Berghmans, H.; Reynaers, H. *Macromolecules* 2004, 37, 9673.
- Rufino, E. S.; Monteiro, E. C. *Polymer* 2000, 41, 4213.
- Scofield, J. H. *J Electron Spectrosc Relat Phenom* 1976, 8, 129.
- Beamson, G.; Briggs, D. *High Resolution XPS of Organic Polymers*; Wiley: UK, 1992.
- Galvan, A.; Ureña, F.; Flores, H.; López, R. *J Appl Polym Sci* 1999, 74, 995.
- Vilchis-Nestor, A. R. B.Sc. Thesis, Facultad de Química, Universidad Autónoma del Estado de México, México, 2000.
- Reichmans, E.; Curtis, W. F.; O'Donnell J. H.; Hill D. J. In *Irradiation of Polymeric Materials. Process, Mechanism and Application*; Reichmans, E.; Curtis, W. F.; O'Donnell J. H., Eds.; ACS: Washington, 1993; Chapter 1.
- Sakai, Y. *J Polym Sci Part A-1: Polym Chem* 1969, 7, 3177.
- Ichikawa, T. *Nucl Instrum Methods Phys Res Sect B* 1995, 105, 150.
- Tannenbaum, R.; King, S.; Lecy, J.; Tirrell, M.; Potts, L. *Langmuir* 2004, 20, 4507.
- Tan, B. J.; Klabunde, K. J.; Sherwood, P. M. *J Am Chem Soc* 1991, 113, 855.
- Socrates, G. *Infrared Characteristic Group Frequencies Tables and Charts*; Wiley: UK, 1994.
- Nakamoto, K. *IR and Raman Spectra of Inorganic Coordination Compounds, Part B: Applications in Coordination, Organometallic and Bioinorganic Chemistry*; Wiley: New York, 1997.
- McCluskey, P. H.; Snyder, R. L.; Condrate, R. A. *J Solid State Chem* 1989, 83, 332.
- Kimura, Y.; Furukawa, M.; Yamane, H.; Kitao, T. *Macromolecules* 1989, 22, 79.

35. Kimura, Y.; Sugaya, S.; Ichimura, T.; Taniguchi, I. *Macromolecules* 1987, 20, 2329.
36. Leman, J. T.; Braddock-Wilking, J.; Coolong, A. J.; Barron, A. R. *Inorg Chem* 1993, 32, 4324.
37. Barron, A. R.; Bethley, C. E.; Aitken, C. L.; Harlan, J.; Koide, Y. *Organometallics* 1997, 16, 329.
38. Barron, A. R.; Koide, Y. *Organometallics* 1995, 14, 4026.
39. Deacon, G. B.; Philips, R. J. *Coord Chem Rev* 1980, 33, 227.
40. Lambert, B.; Shurvell, F.; Lightner, A.; Cooks, G. *Organic Structural Spectroscopy*; Prentice Hall: USA, 1998.
41. Silverstein, R. M. *Spectrometric Identification of Organic Compounds*; Wiley: USA, 1998.
42. Pouchert, C. J. *The Aldrich Library of Infrared Spectra*, 3rd ed.; Aldrich Chem Company: USA, 1981.
43. Nyquist, R. A.; Putzig, C. L.; Leugers, M. A. *Handbook of Infrared and Raman Spectra of Inorganic Compounds and Organic Salts*, Vol. 1; Academic Press: USA, 1997.
44. Srinivasan, S.; Narayanan, C. R.; Datye, A. K. *Appl Catal A* 1995, 132, 289.
45. Landry, C.; Pappé, N.; Mason, M.; Apblett, A.; Tyler, A.; MacInnes, A.; Barron, A. R. *J Mater Chem* 1995, 5, 331.
46. Gurian, P. L.; Cheatham, L. K.; Ziller, J. W.; Barron, A. R. *J Chem Soc Dalton Trans* 1991, 1449.
47. Cotton, A. F.; Wilkinson, G. *Advanced Inorganic Chemistry*; Limusa: México, 2001.
48. McNeill, I. C.; Zulfiqar, M. *J Polym Sci Polym Chem Ed* 1978, 16, 2465.
49. Zulfiqar, S.; Masud, K. *Polym Degrad Stab* 2002, 78, 305.